Experimental Demonstration of Quantitative Imaging beyond Abbe's Limit with Optical Diffraction Tomography

Guillaume Maire,[1,2] Filip Drsek,[1,2] Jules Girard,[1,2] Hugues Giovannini,[1,2] Anne Talneau,[3] Denis Konan,[4] Kamal Belkebir,[1,2] Patrick C. Chaumet,[1,2] and Anne Sentenac[2]

[1]*Universités d'Aix-Marseille I & III, Marseille, France*
[2]*CNRS, Institut Fresnel, Campus de Saint Jérôme 13013 Marseille, France*
[3]*CNRS, Lab Photon & Nanostruct, 91460 Marcoussis, France*
[4]*Institut National Polytechnique Houphouët Boigny BP 1083 Yamoussoukro, Ivory Coast*

(Received 25 August 2008; revised manuscript received 1 April 2009; published 29 May 2009)

Optical diffraction tomography (ODT) is a recent imaging technique that combines the experimental methods of phase microscopy and synthetic aperture with the mathematical tools of inverse scattering theory. We show experimentally that this approach permits us to obtain the map of permittivity of highly scattering samples with axial and transverse resolutions that are much better than that of a microscope with the same numerical aperture.

DOI: 10.1103/PhysRevLett.102.213905 PACS numbers: 42.30.Wb, 42.25.Fx

There has been a considerable recent interest in the development of new optical imaging systems that are able to give the three-dimensional optical properties of a sample, as encoded in the spatial variations of the permittivity, at the nanoscale [1–3]. Potential applications range across multiple fields in life and material science. For instance, in nanofabrication, one important objective is to control the manufacturing of heterogeneous stacked platforms with typical length scales about 100 nm. In biology, the study of the inner structure of unstained cells is recognized as increasingly important [4]. Standard optical microscopes do not provide quantitative information on the sample permittivity [5] as crucial information is lost when sole the intensity of the field diffracted by the sample is detected. Moreover, their resolution is limited by Abbe's criterion and becomes too low in numerous applications. To circumvent these two difficulties, it has been proposed to measure the field in the near vicinity of the sample and to use an inversion algorithm to reconstruct the permittivity of the object from the complex-valued data [1,6]. Though full of promises, this approach is experimentally challenging and the observed transverse resolution remained close to that of a conventional microscope. Another technique, simpler from an experimental point of view, consists in measuring the diffracted field in a far-field microscope for many incident angles [4,7–11]. An inversion algorithm is then used to form the image from the multiple data set. This approach, generically known as optical diffraction tomography (ODT) or synthetic aperture digital holography, has stirred a wealth of research in the last five years and various setups, adapted to biological applications [4,8,11] or to surface imaging [7,9,10] were proposed.

In all these pioneering experimental works, the model for the wave-object interaction is based on the single-scattering assumption. This assumption is widespread in most tomographic imaging systems, from the acoustical to the x-ray domains, as it yields fast and simple linear inversion algorithms. Yet, it is valid only for weakly scattering objects or specific geometries and it cannot be applied to samples presenting high or moderate permittivity contrasts, such as those encountered in the nanofabrication domain. Hence, an important field of applications is still out of reach of this new imaging tool.

In this work, we develop an ODT setup that operates with a nonlinear inversion algorithm accounting for multiple scattering. We show experimentally that this approach can provide the map of permittivity of highly scattering nanostructures with an axial and transverse resolutions far beyond that of an analogical microscope or that obtained with the commonly used linear inversion procedures.

The principles of ODT [7–11] is depicted in Fig. 1. The sample is illuminated by a monochromatic plane wave with wavelength λ and the reflected scattered far field is detected for various observation angles θ_d varying between

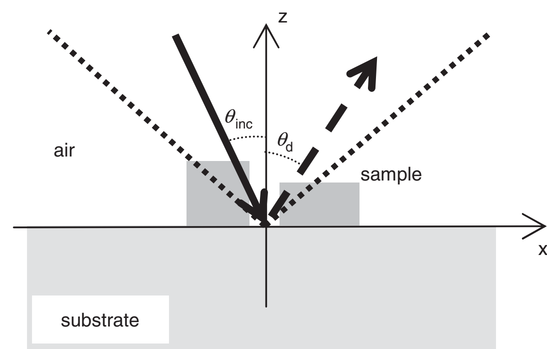

FIG. 1. Schematic view of an ODT experiment in a reflection configuration. θ_{inc} is the angle of the incident illumination on the sample, θ_d is the angle indexing the diffraction directions. The dotted lines indicate the numerical aperture of the objective that collects the diffracted light.

 © 2009 The American Physical Society

$[\pm\theta_{d_{\max}}]$. To increase the resolution of the system, multiple sets of scattered far-field are recorded for different incident angles θ_{inc} varying between $[\pm\theta_{\text{inc}_{\max}}]$.

The experimental setup is basically a conventional reflection microscope which has been modified to allow the measurement of the phase of the diffracted field and the successive illumination of the sample under various incident angles (Fig. 2). Note that in a reflection microscope, the sample is also illuminated under various incident angles though in a simultaneous (and incoherent) manner.

The emitted light at 633 nm by a 10 mW Helium-Neon laser is divided into a reference beam, passing through an electro-optic phase modulator, and a signal beam directed towards the sample. The latter illuminates the sample with a collimated beam over a wide range of incidence angles (typically $\pm 32°$) and with a homogeneous intensity.

The field diffracted by the object is collected by the microscope objective L_1 (Zeiss "Fluar"×20 with a numerical aperture NA = 0.75 in the air). An intermediary image of the sample is obtained at the object focal plane of L_4, where a field diaphragm D_2 permits to adjust the field of view without changing the diameter of the illumination beam. The diffracted field and the reference field are superimposed coherently thanks to beam splitter B_3. A digital hologram of the diffracted field is then recorded in the Fourier plane on a charge-coupled device (CCD) camera (758 × 568 pixels) by phase-shifting interferometry thanks to phase modulator (PM) [12]. The CCD camera also detects the specular reflection of the incident beam on the sample substrate. The amplitude and phase matching of the fields over the different incidences is performed through a normalization that ensures that each specularly reflected field is equal to the theoretical complex reflectivity of the bare substrate. This implies that the permittivity of the substrate is known and that the amplitude of the diffracted field is negligible as compared to that of the specular beam [8]. This assumption is verified even for strongly scattering samples if the overall size of the scattering objects is small compared to that of the field of view.

Once the digital holograms are recorded in the Fourier plane for all incidences, the image of the sample is reconstructed by a numerical procedure. The simplest algorithm, that is used in most ODT surface imaging [7,9,10], amounts to joining all the holograms into a global set of data and performing a 2D inverse Fourier transform. This linear inversion procedure relies on an approximate modelization of the field existing at the object focal plane of the microscope, that is,

$$E(\boldsymbol{r}_\parallel) = R(\boldsymbol{r}_\parallel)E_{\text{inc}}(\boldsymbol{r}_\parallel), \tag{1}$$

where $\boldsymbol{r}_\parallel = (x, y)$, R is the reflectance of the structured sample, and E_{inc} is the incident field [7]. Under this approximation, the hologram obtained in the Fourier plane at the reciprocal variable $\boldsymbol{k}_\parallel$ is proportional to $\tilde{R}(\boldsymbol{k}_\parallel - \boldsymbol{k}_{\parallel\text{inc}})$, where $\tilde{R}$ is the 2D Fourier transform of R and $\boldsymbol{k}_{\parallel\text{inc}}$ is the transverse wave vector of the incident plane wave. Hence, the use of several incidences permits us to enlarge the accessible domain of spatial frequencies of R. As a result, the power of resolution of the reconstructed image with ODT is much better than that obtained with single incidence holography. It should be, in principle, also better than that obtained with wide-field microscopy with incoherent illumination because ODT does not dim the accessible highest spatial frequencies of the object contrary to analogical microscopy [5,7]. In this work, we have replaced this ODT classical linear inversion algorithm (ODT-LIA) by a nonlinear reconstruction algorithm that is based on a rigorous model of the light-sample interaction. Our approach permits the retrieval, quantitatively, of the map of permittivity of the sample in the transverse and axial directions from the measured holograms.

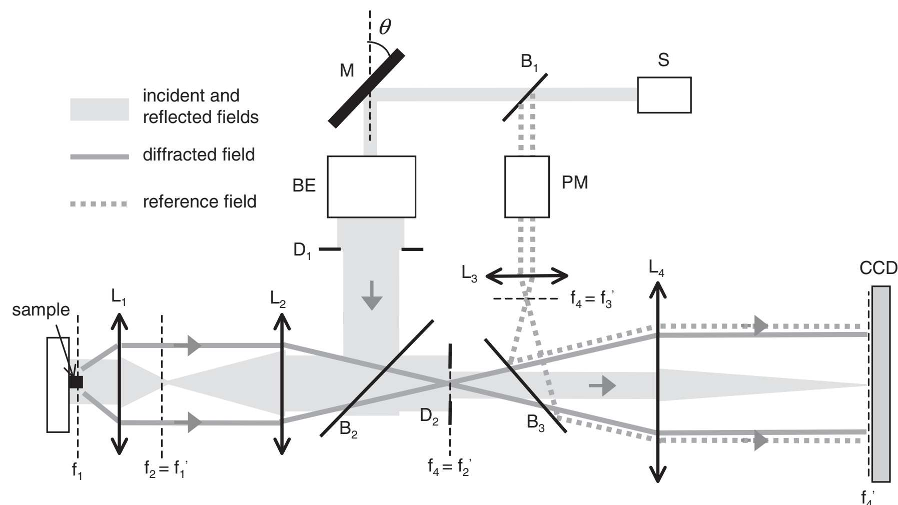

FIG. 2. Sketch of the experimental setup. L_1, L_2, L_3, L_4, lenses; f_i and f'_i, associated object and image focal planes; S, laser source emitting at 633 nm; M, adjustable mirror; B_1, B_2, B_3, beam splitters; BE, beam expander; PM, phase modulator; D_1, D_2, diaphragms.

We considered samples that are invariant along the y axis and illuminated by an incident plane wave with a wave vector belonging to the plane normal to $\hat{y}$ with an electric field directed along $\hat{y}$ (see Fig. 1). In this case, the diffraction problem is scalar. We use the *a priori* information that the sample is made of lossless dielectric objects deposited on a substrate with known permittivity. The complex amplitude of the total field directed along $\hat{y}$ can be written as [13],

$$E(x, z) = E_{\text{ref}}(x, z) + \int G(x - x', z, z')\chi(x', z')E(x', z')dx'dz', \quad (2)$$

where E_{ref} is the field that would exist without the objects, $G(x - x', z, z')$ denotes the field at (x, z) radiated by a line source placed at (x', z') above the substrate and $\chi(x', z') = 1 - \varepsilon(x', z')$ is the permittivity contrast which is nonzero only in the objects. Equation (2) can be used in the far-field zone to describe the scattered field measured in the Fourier plane and in the near-field zone to estimate the field inside the objects. If single scattering and paraxial approximation are assumed, Eq. (2) reduces to Eq. (1) and the scattered far field is related to only one spatial frequency of the sample reflectance. Outside these conditions, it can be shown from Eq. (2) that the scattered far-field depends, in a complex way, on all the object spatial frequencies [14,15]. While the latter cannot be unraveled explicitly, several works have pointed out that inversion algorithms based on a rigorous simulation of the diffracted field could give images containing spatial frequencies above that given by the single-scattering analysis [15–18].

To reconstruct the permittivity map of the sample, we developed a nonlinear inversion algorithm [13] in which χ, restricted to a bounded investigating domain above the substrate, is updated gradually by minimizing a cost function that describes the discrepancy between the measured scattered far-field and the simulated one. Multiple scattering within the sample is taken into account by computing rigorously at each iteration step the field inside the investigating domain. We have considered several samples consisting in parallel rods of resin, with rectangular cross-sections, deposited on a silicon substrate. The relative permittivity of the silicon and the resin is $\varepsilon = 15.07$ and $\varepsilon = 2.66$, respectively. We used 10 incidences with angles θ_{inc} varying between $\pm\theta_{\text{inc}_{\max}} = 32°$ and collected the scattered field for about 600 observation angles θ_d ranging between $\pm\theta_{d_{\max}} = 46°$. With such incident and collection numerical apertures, the Abbe limit is given by $\lambda/(\sin\theta_{\text{inc}_{\max}} + \sin\theta_{d_{\max}}) \approx 500$ nm.

The first sample (Fig. 3) is made of two rods of height 140 nm and widths 1 μm and 500 nm, separated by 500 nm. The second sample (Fig. 4), consists of three rods of height 110 nm and width 200 nm separated by 300 nm. The third sample (Fig. 5) is similar to the second one except that the rod width is 100 nm. Figures 3(a), 4(a), and 5(a) show the profile of the rods as measured by an atomic force microscope. For the three samples, we plot the intensity given by a standard wide-field microscope with NA = 0.75 and enlargement ×100, the squared modulus of the reflectance given by the standard inverse

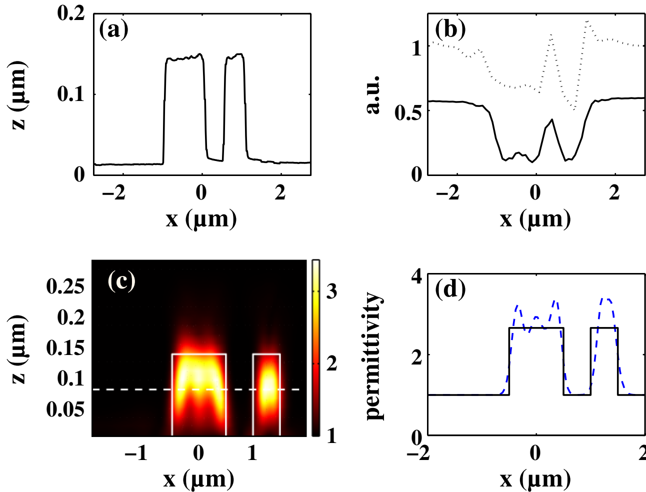

FIG. 3 (color online). The sample is constituted of two rectangular rods of resin deposited on a silicon substrate. The rods height is 140 nm and their widths are 1 μm and 500 nm. The rods are separated by 500 nm side to side. (a) Height profile provided by the AFM. (b) Dotted line: squared modulus of the reflectance obtained with ODT-LIA approach [7]. Solid line: Intensity measured at the image plane of a wide-field optical microscope with NA = 0.75 and red incoherent light. (c) Map of the permittivity obtained with the Non-Linear Inversion Algorithm applied to the same data as that used in the ODT-LIA approach. (d) Comparison along the dashed line plotted in (c) of the reconstructed permittivity (dashed line) with the actual value (solid line).

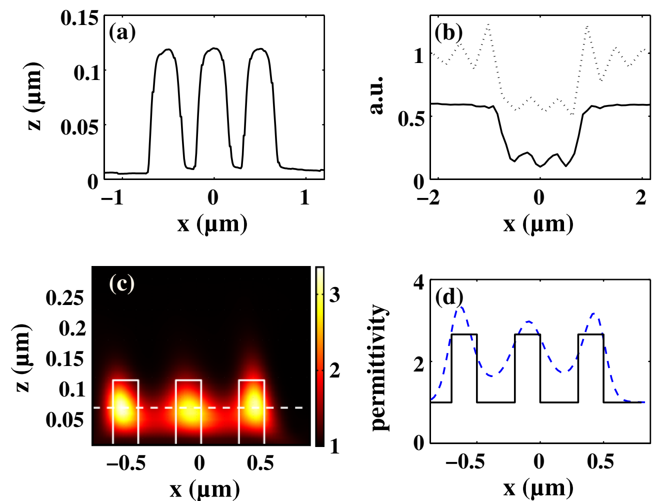

FIG. 4 (color online). Same as Fig. 3 except that the sample is constituted of three identical resin rods of height 110 nm and width 200 nm separated by 300 nm side to side.

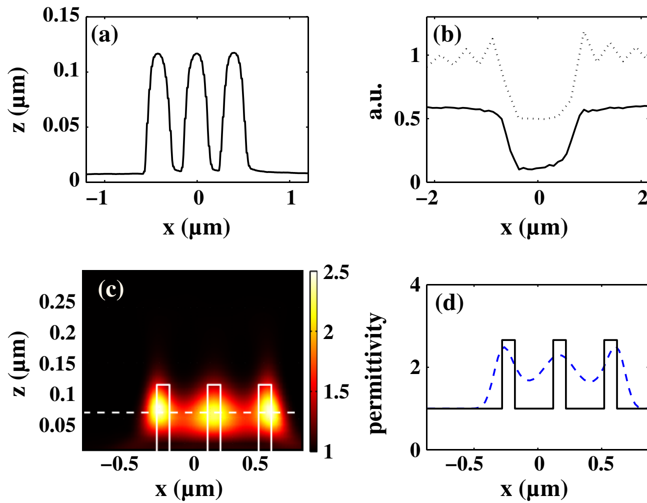

FIG. 5 (color online). Same as in Fig. 4 but the rods width is 100 nm.

Fourier algorithm, and the map of permittivity given by the nonlinear inversion algorithm.

We observe that, in all examples, the power of resolution of ODT-LIA is similar to that of the wide-field microscopy while it is clearly outperformed by the same ODT approach combined with the Non-Linear Inversion Algorithm (ODT-NLIA). The disappointing performances of ODT-LIA, as compared to those of the wide-field microscope, stem mainly from the Gibbs phenomenon and the strong sensitivity to the data noise that deteriorate the reconstructed reflectance.

The superiority of the ODT-NLIA is particularly blatant in Fig. 5 where the center interdistance of the rods, equal to 400 nm is smaller than the Abbe limit. Indeed, ODT-LIA fails to separate the rods [Fig. 5(b)], contrary to the ODT-NLIA [Fig. 5(d)]. In this last case, the separation between the rods is so marked that it is likely that 400 nm is not the ultimate resolution of the imager. In our opinion, the significant improvement brought by the ODT-NLIA is essentially due to the fact that, first, it takes advantage of the *a priori* information that the objects are deposited on a known substrate and that their permittivity is positive; second, it is based on a rigorous calculation of the diffracted field so that it is not plagued by any model error and it has potentially access to spatial frequencies that are higher than that given by the single-scattering analysis.

Note that, besides the gain in transverse resolution, the ODT-NLIA is also able to estimate the height of the objects with a high sensitivity: the 30 nm difference between the heights of the rods in Figs. 3–5, is clearly visible on the reconstructed map of permittivity.

In conclusion, we believe that combining ODT with inversion algorithms resorting to accurate modeling of the wave-object interaction is a promising path for high resolution quantitative imaging of complex objects. The quantitative information provided by this kind of imager (permittivity distribution with high axial and transverse resolutions), is, to our knowledge, out of reach of all present imaging systems. Sub-100 nm resolution in both axial and transverse directions is expected with the latest objectives presenting a numerical aperture of about 1.5, or with the recently proposed grating-assisted ODT approach [2]. Note that digital imaging should be all the more interesting now that computation facilities are increasing.

[1] P. S. Carney, R. A. Frazin, S. Bozhevolnyi, V. S. Volkov, A. Boltasseva, and J. C. Schotland, Phys. Rev. Lett. **92**, 163903 (2004).
[2] A. Sentenac, P. C. Chaumet, and K. Belkebir, Phys. Rev. Lett. **97**, 243901 (2006).
[3] Z. Liu, H. Lee, Y. Xiong, C. Sun, and X. Zhang, Science **315**, 1686 (2007).
[4] W. Choi, C. Fang-Yen, K. Badizadegan, S. Oh, N. Lue, R. Dasari, and M. Feld, Nat. Methods **4**, 717 (2007).
[5] N. Streibl, J. Opt. Soc. Am. A **2**, 121 (1985).
[6] G. Y. Panasyuk, V. A. Markel, P. S. Carney, and J. C. Schotland, Appl. Phys. Lett. **89**, 221116 (2006).
[7] S. A. Alexandrov, T. R. Hillman, T. Gutzler, and D. D. Sampson, Phys. Rev. Lett. **97**, 168102 (2006).
[8] V. Lauer, J. Microsc. **205**, 165 (2002).
[9] A. Neumann, Y. Kuznetsova, and S. R. Brueck, Opt. Express **16**, 6785 (2008).
[10] V. Mico, Z. Zalevsky, P. Garcia-Martinez, and J. Garcia, J. Opt. Soc. Am. A **23**, 3162 (2006).
[11] M. Debailleul, B. Simon, V. Georges, O. Haeberlé, and V. Lauer, Meas. Sci. Technol. **19**, 074009 (2008).
[12] I. Yamaguchi and T. Zhang, Opt. Lett. **22**, 1268 (1997).
[13] K. Belkebir and A. Sentenac, J. Opt. Soc. Am. A **20**, 1223 (2003).
[14] C.-A. Guérin and A. Sentenac, J. Opt. Soc. Am. A **21**, 1251 (2004).
[15] F. Simonetti, Phys. Rev. E **73**, 036619 (2006).
[16] F. C. Chen and W. C. Chew, Appl. Phys. Lett. **72**, 3080 (1998).
[17] K. Belkebir, P. C. Chaumet, and A. Sentenac, J. Opt. Soc. Am. A **23**, 586 (2006).
[18] A. Sentenac, C.-A. Guérin, P. C. Chaumet, F. Drsek, H. Giovannini, N. Bertaux, and M. Holschneider, Opt. Express **15**, 1340 (2007).